ChemComm

Accepted Manuscript

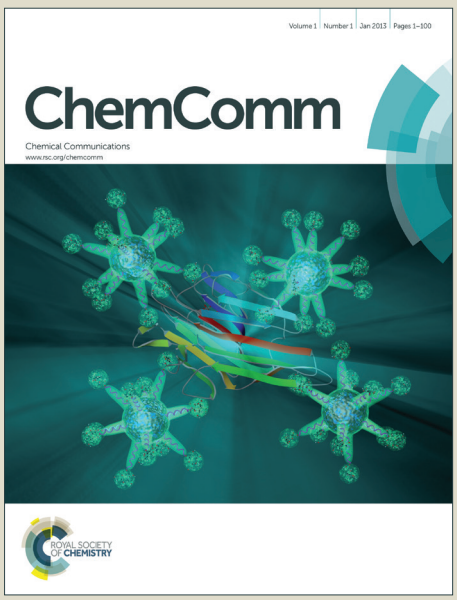

This is an *Accepted Manuscript*, which has been through the Royal Society of Chemistry peer review process and has been accepted for publication.

Accepted Manuscripts are published online shortly after acceptance, before technical editing, formatting and proof reading. Using this free service, authors can make their results available to the community, in citable form, before we publish the edited article. We will replace this *Accepted Manuscript* with the edited and formatted *Advance Article* as soon as it is available.

You can find more information about *Accepted Manuscripts* in the Information for Authors.

Please note that technical editing may introduce minor changes to the text and/or graphics, which may alter content. The journal's standard Terms & Conditions and the Ethical guidelines still apply. In no event shall the Royal Society of Chemistry be held responsible for any errors or omissions in this *Accepted Manuscript* or any consequences arising from the use of any information it contains.

ROYAL SOCIETY OF CHEMISTRY

www.rsc.org/chemcomm

Cite this: DOI: 10.1039/c0xx00000x

www.rsc.org/xxxxxx

ARTICLE TYPE

First observation to enhanced luminescence from single lanthanide chelate on silver nanorod

Jian Zhang, *Krishanu Ray, Yi Fu, and Joseph R. Lakowicz

Received (in XXX, XXX) Xth XXXXXXXXX 20XX, Accepted Xth XXXXXXXXX 20XX

DOI: 10.1039/b000000x

We used a near-field interaction with a silver nanorod (AgNR) to greatly enhance luminescence of a lanthanide (Ln) chelate. The enhancement factor was 280-fold leading to single lanthanide luminescence detectable. This is also the first observation on single molecule detection (SMD) of a lanthanide dye.

Single molecule detection (SMD) techniques can be used to explore the optical properties from single fluorophores in heterogeneous samples. [1,2] To record the emission signal from a single fluorophore, alone the background emission, the fluorophore must have a relatively high emission brightness. Currently, the detection background can be efficiently supressed using confocal microscope. [3] But increased emission brightness of the fluorophore is severely limited by its chemical structure which cannot be easily altered. [4,5] As a result, only selected organic fluorophores can be sued for SMD.

As luminescent dyes, lanthanides (Lns) are attracting a wide research interest because of their excellent optical properties including extremely large Stokes shifts, narrow spectra, and long lifetimes. [6,7] When the Ln dyes are used as contrast agents for fluorescence imaging and bioassays, the short-lifetime emission backgrounds can be efficiently rejected with time-gated methods and, as a result, the long-lifetime emissions from the Ln dyes can be detected with high sensitivity. [8] However, the Ln dyes have significant weakness on their optical properties. Basically, the emission from Ln ion may involve an electron transition in a 4f orbital which is forbidden. Consequently, the Ln ion usually displays extremely slow excitation and emission rates leading to its low absorbance coefficient and slow radiative rate. [12] The Ln ion hence emits a very low luminescence. To increase the emission intensity, the Ln ion is often coordinated with organic ligands to form chelate. [7,8] The ligands in the chelate can sufficiently absorb the excitation light and subsequently transfer the energy to the Ln centre. Compared to the Ln ion, the Ln chelate often has an absorption coefficient several orders of magnitude higher leading to that the Ln chelate becomes much brighter. But on the other side, the coordination cannot increase the emission rate of Ln centre so that the improvement of its optical properties is severely limited. Actually, compared with the organic fluorophores, the Ln chelates are often found to emit a lower brightness. Importantly, we notice that under the current conditions, there is still lack of a report on the SMD using the Ln dyes.

In the past decade, near-field interactions have been widely employed to increase the excitation and emission rates of a fluorophore and, furthermore, enhance its fluorescence intensity, extend its photobleaching time, and reduce its photoblinking. [9,10] Basically, the irradiation of a subwavelength size metal nanoparticle with the light can create a high local electric field. Placement of a fluorophore in this local field within a near-field distance from the metal nanoparticle can result in significant increases in the excitation or/and emission rates of the fluorophore. As a result, fluorescence from the fluorophore can be significantly enhanced from several to thousand folds due to

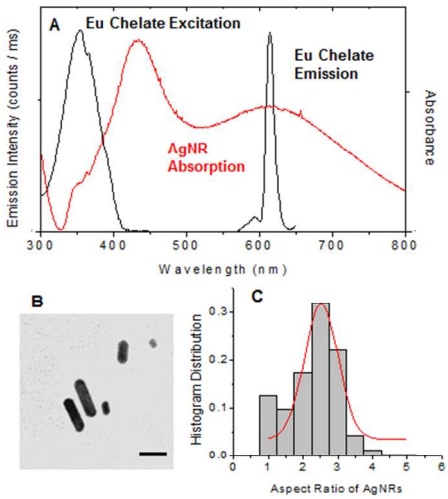

Fig.1. (a) Absorption spectra (red) of AgNRs and excitation and emission spectra of Eu chelates (black) in the silica templates in aqueous solution. The excitation spectrum was collected by monitoring the emission at 615 nm. The emission spectrum was obtained upon excitation at 375 nm. The ensemble excitation and emission spectra were acquired with a time-gated method. The delay time and decay time were adjusted to 0.1 ms and 5 ms, respectively. (b) TEM images of AgNRs. The scale bar is 20 nm. (c) Histogram distribution showing aspect ratios for the AgNRs. Most AgNRs were observed to have an average width of15 nm and length of 38 nm.

the near-field interactions. [10] There have been many reports on the near-field interaction studies. [9-13] But it is also noticed that these reports mostly focus on the organic fluorophores and quantum dots, and only few on the Ln dyes. [14,15] It is because the organic fluorophores and quantum dots display relatively small Stokes shifts so the excitation and emission spectra of them can sufficiently couple the single plasmon band from the metal

ChemComm Accepted Manuscript

nanospheres, which are generally adopted for the near-field interaction studies, to achieve efficient fluorescence enhancement. In contrast, the Ln dyes display very large Stokes shifts and the excitation and emission spectra of Ln dyes cannot sufficiently couple the single plasmon band from the metal nanospheres. Consequently, the luminescence of Ln dyes cannot be efficiently enhanced on the metal spheres by the near-field interactions.

In a recent paper of us, we reported ensemble measurements of silver nanorods (AgNRs) coupled with the europium (Eu) chelates for enhancing the luminescence of Eu chelates. [16] The AgNRs displayed dual-mode plasmons from the transverse and longitudinal axis, respectively, approximately matching the excitation and emission spectra of the Eu chelates. The Eu chelates hence could efficiently couple with the AgNRs at both the excitation emission leading to a great luminescent enhancement. The enhancement factor was observed to reach to 240-fold. On the other hand, we immobilized hundreds of Eu chelates on one AgNR and conducted measurements of optical properties using ensemble spectral method. The SMD of Ln dye was still lacking. In this communication, we control the experiment conditions to tether the single Eu chelate on per AgNR. The AgNRs were also fabricated to display dual-mode plasmons more precisely matching the excitation and emission from the Eu chelates. As a result, a larger near-field interaction was expected to achieve and fluorescence from the Eu chelate was enhanced in a larger scale leading to that the emission signal from the single Eu chelate could be observed.

Typically, in a seed-mediated growth method as described early,

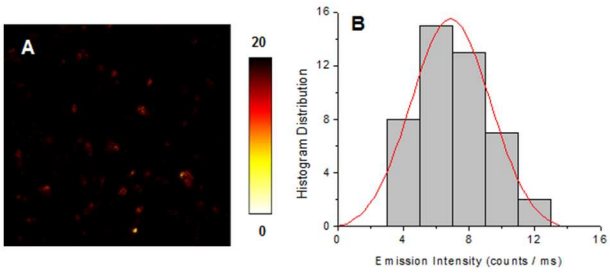

Fig.2. (a) Upon excitation at 375 nm with a frequency of 5 MHz, a fluorescence intensity image of Eu-AgNR complexes was collected from the emission through a 610±35 nm bandpass filter. The area of image is 5 x 5 μm and the resolution of image was 400 x 400 pixel with an integration of 0.6 ms / pixel. (b) Histogram distribution of emission intensities from the individual Eu-AgNR complexes.

[15] the AgNRs in the current study were fabricated to display dual-mode plasmon absorptions centred at 415 nm and 610 nm from transverse and longitudinal axis, respectively, and the longitudinal plasmon from the current AgNRs was found to precisely match the emission spectrum of the Eu chelates (Fig.1a). From the TEM images (Fig.1b), about 200 individual AgNRs were selected to estimate their aspect ratios. The data were collected and analysed by fitting with a Gaussian distribution model (Fig.1c) showing a maximum at 2.5. Thus, these AgNRs were achieved to have an average width of 15 nm and length of 38 nm.

To immobilize the Eu chelates on the AgNRs, the silica shells were deposited as thin layers on the external surfaces of AgNRs via a hydrolysis reaction of tetraethyl orthosilicate. To ensure that the Eu chelates were immobilized within a near-field distance from the AgNRs, the silica shells were controlled to be 5 nm thick on the AgNRs. The Eu chelates were absorbed into the silica shells from solution. Typically, the Eu chelate was dissolved in an ethanol solution containing the silica-AgNR nanoparticles at a molar ratio of Eu chelate/AgNR =1/20. In this solution, the silica-coated AgNR was in a largely excess amount relative to the Eu chelate. So the Eu chelates were mostly absorbed as single chelate on one AgNR. Experimental details can be found in the **Supplementary Material**.

To exp-lore the effort of the AgNR to the luminescence of Eu chelate, a NaCN treatment was used to dissolute the metal from the Eu-AgNR complexes. [16] Typically, several drops of 0.1 M NaCN solution was added to a Eu-AgNR complex solution. With dissolution of AgNRs by NaCN, the Eu-silica templates were

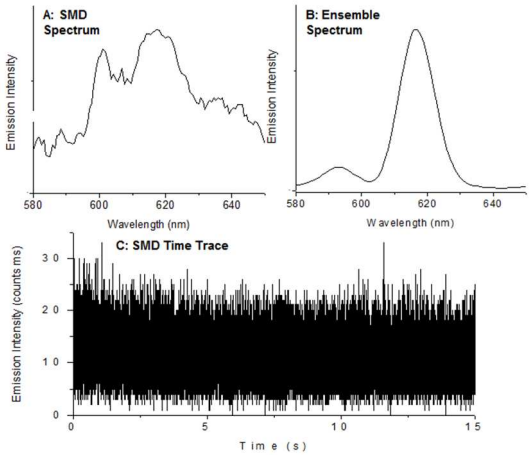

Fig.3. (a) Emission spectrum from single Eu-AgNR complex was collected upon excitation at 375 nm with a frequency of 5 MHz. (b) Ensemble emission spectrum was collected up on excitation at 375 nm with a time-gated method. The delay time and decay time were adjusted to 0.1 ms and 5 ms, respectively. (c) Intensity time-trace from a single emission spot on Fig.2a.

released as metal free into solution. The emission intensity from the Eu chelates was observed to reduce with the metal dissolution (Fig.S1). To explore the possible influence from the NaCN itself to the change of luminescence in this treatment, the ensemble emission spectrum from the Eu-silica nanoparticles was monitored by adding serial concentration of NaCN to the solution. The emission spectrum displayed insignificant decrease indicating that the emission from the Eu chelates in the silica nanoparticles could not be influenced by the NaCN. Thus, it was predicted that the decreased emission intensity of the Eu-AgNR complexes in the NaCN treatment was due to the dissolution of AgNRs and the loss of near-field interactions. According to the ratio of emission intensity prior to the treatment to that after the treatment, the enhancement factor was estimated to be 280-fold. This value is larger than the enhancement factor for the same Eu chelates on the AgNRs as our early report. [16] It could be ascribed to more sufficient spectral overlap between the emission of Eu chelate and longitudinal plasmon of AgNR. This value is also larger than the enhancement factors for most organic fluorophores on the single metal nanoparticles, [10] suggesting that the Eu chelates can efficiently couple on the AgNRs.

Next, we examined the emission signals from the individual Eu-AgNR complexes with a stage-scanning confocal microscope. First, the Eu-AgNR complex-containing solution with nM

ChemComm Accepted Manuscript

This journal is © The Royal Society of Chemistry [year]

concentration was cast on a glass coverslip and subsequently dried in air. Herein, we could not provide direct evidence to support that these Eu-AgNR complexes were presented as individuals on the coverslip. However the scanning confocal image in Fig.2a displayed well-separated individual spots resulting from the emission of Eu-Ag NR complex. The intensity histogram (Fig.2b) also expressed a tight distribution of count rate. Both represent that the Eu-AgNR complexes were presented as individuals. In addition, with the similar treatments, the organic fluorophores are found to mostly present as single fluorophores on the coverslips in the fluorescence imaging measurements. [13] We also cast the nM AgNR-containing solution on the grid for the TEM measurements on which the AgNRs were observed to mostly present as individuals (Fig.1b). We also immobilized the Cy5 on the AgNRs in the same strategy. The time traces from the emission spots on the image expressed single-step photobleaching which is typical process from the single fluorophore. Thus, we could predict that the Eu-AgNR complexes should be presented as individuals on the coverslip.

As controls, the nM free Eu chelate and Eu-silica nanoparticle solutions were cast on the coverslips, respectively, and dried in air for the imaging measurements. With the similar concentrations, these Eu samples were also expected to present as single fluorophores or individual nanoparticles.

The Eu samples on the coverslips were excited with a laser of 375 nm and the emission signals were recorded through a 610±35 bandpass filter on the confocal microscope. Since the Eu chelates have extremely long lifetimes, the repetition rate of excitation laser was reduced to a low frequency of 5 MHz. The emissions from the Eu-AgNR complexes were observed as round spots on the image (Fig.2a). In contrast, no emission signal from the free Eu chelates and Eu-silica nanoparticles could be detected.

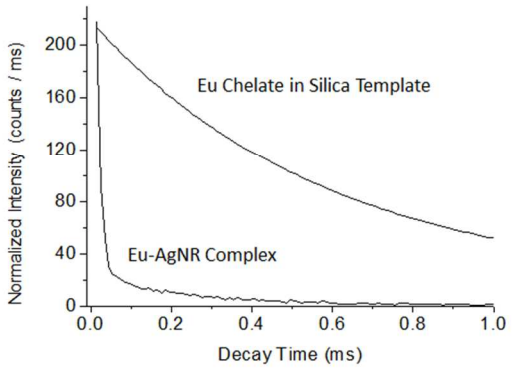

Fig.4. Intensity-decay curves of Eu chelates on the metal-free silica templates and bound on the AgNRs. These decay curves were acquired upon excitation at 375 nm with a time-gated method. The gate pulse width was controlled to be 0.5 ms and the delay time was 0.1 ms.

It was noticed that the emission spots from the Eu-AgNR complexes had relatively low brightness which was mostly below 20 counts / msec. To confirm that they were arisen from the luminescence of Eu chelates, some emission spots in the image was selected to monitor their emission spectra using an Acton spectrograph that was coupled to an EMCCD camera and installed on the microscope (Fig.3a). These spectra were found to be similar to the ensemble spectrum of Eu-AgNR complexes in solution (Fig.3b). We also cast the Eu-free silica-AgNR nanoparticles on the coverslip for collecting their scattering signals under the same conditions. On the image, there was no emission signal distinguishable from the background supporting that the emission spots in Fig.2a were indeed from the Eu chelates. On the basis of these observations, it is concluded that the emissions from the single Eu chelates become detectable on the microscope only when the Eu chelates are immobilized on the AgNRs and the luminescence from these chelates is largely enhanced by the near-field interactions.

It is interesting to notice that the intensity time-traces (Fig.3c) of the emission spots in Fig.2a expressed an apparent monotonic decay instead of a single-step bleaching which is typical behaviour of single fluorophore but. But the emissions from the single Cy5 dyes on the silica-AgNR nanoparticles mostly expressed the typical single-step photobleaching on the time-traces (Fig.S2). [14] Thus, we suggest that the Eu chelates were indeed absorbed on the AgNR as single fluorophores. The monotonic decay from a Eu-AgNR complex was probably due to progressive photocleavage of its ligands with the light irradiation. It is known that fluorescence of Ln centre can be dramatically increased by coordination with the organic ligands. In contrast, with the light irradiation, the coordination ligand in the chelate is expected to photocleavage and, thus, the emission efficiency of Ln centre is reduced leading to a decrease of intensity. In this mechanism, we expect to observe the emission decay from a single Ln chelate with multiple-step photobleaching. However, the emission count rates from the individual spots (Fig.2c) are too low. Correspondingly, the intensity time-traces were also observed to have very low emission count rate leading to that the multiple-step photobleaching becomes an indistinctly apparent monotonic decay.

To further evaluate the emission intensities from the single Eu chelates on the AgNRs, about 50 emission spots in Fig.2a were collected and the intensities were analysed by fitting with a Gaussian distribution model (Fig.2b). From the distribution curve, the maximum of 7 counts / ms was obtained. This value was larger than the intensity of emission background which was below 2 counts / ms. Thus, the emission signals from the single Eu-AgNRs complexes could be identified from the backgrounds. On the other hand, this intensity was relatively low resulting in dim emission spots. Nevertheless, it was first observation to the emission signals from the single Ln dyes which was due to largely enhanced luminescence by the near-field interactions.

The near-field interaction for an excited fluorophore with a metal nanoparticle can increase its radiative rate and bring up a decrease of lifetime. [9,10] From the emission spectral overlap in Fig.1, the lifetime of Eu chelates on the AgNRs should be significantly reduced. The decays from the excited Eu chelates in the silica nanoparticles or on the AgNRs were collected using ensemble solution method (Fig.4). Compared to the Eu chelates in the silica nanoparticles, the chelates on the AgNRs were observed to have a much shorter decay time. The decay curves were analysed in terms of two-exponential model. The average lifetime of Eu chelates was estimated to 0.6 ms in the silica templates, and was dramatically reduced to 15 μs on the AgNRs, about a 40-fold decrease.

For a fluorophore on a metal nanoparticle, the fluorescence enhancement due to the near-field interaction can be considered to contribute from both the excitation and emission interactions.

ChemComm Accepted Manuscript

[10] The total enhancement factor hence can be written as the product of the excitation and emission enhancement. Considering the influence from other factors in the process, the enhanced brightness (Y_{APP}) can be expressed as: [19]

$$Y_{APP} = Y_{ex}\, \gamma_{ex}\, \eta_{coll}\, \sigma \qquad (1)$$

where, γ_{ex} is the metal-induced excitation rate of the fluorophore at the excitation wavelength, γ_{em} is the metal-induced emission rate of the fluorophore at the emission wavelength, η_{coll} is the collection efficiency of the far-field light under the experimental conditions and σ is a normalization factor. For the systems with the similar experiment conditions, the σ and η_{coll} factors should be similar and, thus, can be approximately neglected. The γ_{ex} and γ_{em} factors hence become the dominant factors to enhance the fluorescence. The γ_{ex} factor strongly relies on the absorption coefficient of the fluorophore and the local field intensity near the metal nanoparticle. It means that the excitation interaction is strongly wavelength-dependent. We suggest that increased spectral overlapping can increase the excitation interaction and the largest excitation interaction can occur only when the absorption spectrum of the fluorophore maximally overlaps the plasmon of the metal nanoparticle. In the similar way, the γ_{em} factor is also wavelength dependent. Increased emission interaction by more efficient spectral overlapping can result in simultaneous increase of both radiative and non-radiative rates of the fluorophore. According to our experiences, the increased radiative rate is the dominant factor and the fluorescence is significantly enhanced. [10,20] Thus, we can conclude that more sufficient spectral overlapping between the fluorophore and metal nanoparticle at both the excitation and emission of the fluorophore can bring more efficient near-field interactions and furthermore a larger scale fluorescence enhancement. Compared to the AgNRs in our early report, [16] the current AgNRs displayed more sufficient spectral overlapping with the Eu chelates at the emission (Fig.1a). As a result, the enhancement factor of Eu chelates on the current AgNRs is larger than the early value.

We also intended to know the change of quantum yield of Eu chelates on the AgNRs. Although the fluorescence enhancement by the near-field interactions can be considered to contribute from both the excitation and emission interactions, in reality, it is difficult to separate these contributions from the total. In this study, we approximately represented the enhancement by the emission interactions with the change of lifetime which was 40-fold. Consequently, the enhancement by the excitation-interactions could be estimated to be 7-fold when the total enhancement factor was 280-fold. The absorption coefficient of Eu chelate on the AgNR hence can be considered to increase by 7-fold due to the excitation interaction. In general, the Eu chelates have a quantum yield of *ca*. 0.1. [6,7] The quantum yield of Eu chelates on the AgNRs is estimated to be ca. 0.6.

A large decrease of lifetime for a fluorophore can significantly increase its photon counting rate and, thus, increase its data acquisition speed when recording the emission. It is particularly important for the Ln dyes because they own extremely long lifetimes to ms. On the other hand, the lifetimes of the Eu-AgNRs were found to remain tens μs much longer than several ns of background emission in the measurements. As a result, the time-gated methods can be still used to reject the short-lifetime backgrounds and the long-lifetime emissions from these Ln-metal nanoparticles can be distinguishable using the time-gated methods. Therefore, the detection sensitivity should be high.

Conclusions+

In this work, we report the first observation of emissions from the single Eu chelates on the AgNRs. This was accomplished by efficient coupling of the excitation and emission spectra of Eu chelates with the dual-mode plasmons of AgNRs leading to largely enhanced luminescence. For future works, we expect to fabricate the Ln-AgNR complexes on the basis of this observation. A large number Ln chelates can be loaded on one AgNR. These Ln-metal nanoparticles will have superior brightness. By reduced lifetimes, they will also have increased data acquisition rates. Meanwhile, the Ln-metal nanoparticles will remain their lifetime much longer than the ns emission backgrounds in the measurements so that their emissions can be detected using time-gated methods leading to high detection sensitivity. Nevertheless, as novel luminescent nanoparticles, the Ln-metal nanoparticles have great potential for biological and medical applications.

Notes and references

[a] *Centre for Fluorescence Spectroscopy, University of Maryland School of Medicine, Department of Biochemistry and Molecular Biology, 725 West Lombard Street, Baltimore, MD 21201. Fax: 4107067500; Tel: 4107067500; E-mail: jzhang@som.umaryland.edu*

The authors would like to appreciate the support by grants from National Institutes of Health (NIH) Grants AI087968 (K.R.) and EB006521 (J.R.L.)

† Electronic Supplementary Information (ESI) available: [details of any supplementary information available should be included here]. See DOI: 10.1039/b000000x/

1. B. Lounis, and W. E. Moerner, *Nature* 2000, **407**, 491.
2. F. Kulzer, and M. Orrit, *Annu. Rev. Phys. Chem.* 2004, **55**, 585.
3. W. E. Moerner, and D. P. Fromm, *Rev. Sci. Instrum.* 2003, **74**, 3597.
4. M. Sameiro, and T. Gonçalves, *Chem. Rev.* 2009, **109**, 190.
5. J. R. Lakowicz, Principles of fluorescence spectroscopy 3rd ed, Kluwer Academic / Plenum Published, New York, 2006.
6. J.-C. G. Bünzli, *Chem. Rev*. 2010, **110**, 2729.
7. K. Binnemans, *Chem. Rev*. 2009, **109**, 4283.
8. M. Y. Berezin, and S. Achilefu, *Chem. Rev*. 2010, **110**, 2641.
9. A. M. Schwartzberg, and J. Z. Zhang, *J. Phys. Chem. C* 2008, **112**, 10323.
10. J. R. Lakowicz, *Anal. Biochem*. 2005, **337**, 171.
11. N. J. Halas, S. Lal, W.-S. Chang, S. Link, and P. Nordlander, Ch*em. Rev*. 2011, **111**, 3913.
12. P., K. Jain, X. Huang, I. H. El-Sayed, and M. A. El-Sayed, *Acc. Chem. Res.* 2008, **41**, 1578.
13. J. Zhang, Y. Fu, M. Chowdhury, and J. R. Lakowicz, *J. Phys. Chem. C* 2008, **112**, 18.
14. Y. Wang, J. Zhou, and T. Wang, *Mater. Lett*. 2008, **62**, 1937.
15. F. Zhang, G. B. Braun, Y. F. Shi, Y. C. Zhang, X. H. Sun, N. O. Reich, D. Y. Zhao, and G. Stucky, *J. Am. Chem. Soc.* 2010, **132**, 2850.
16. J. Zhang, Y. Fu, K. Ray, Y. Wang, and J. R. Lakowicz, *J. Phys. Chem. C* 2013, **117**, 9372.
17. M. Seitz, E. G. Moore, A. J. Ingram, G. Muller, and K. N. Raymond, *J. Am. Chem. Soc*. 2007, **129**, 15468.
18. T. Ming, L. Zhao, Z. Yang, H. Chen, L. Sun, J. Wang, and C.Yan, *Nano Lett*. 2009, **9**, 3896.
19. Y. Chen, K. Munechika, and D. S. Ginger, Nano Lett. 2007, 7, 690.
20. O. L. Muskens, V. Giannini, J. A. Sánchez-Gil, and J. Gómez Rivas, Nano Lett. 2007, 7, 2871.

ChemComm Accepted Manuscript

This journal is © The Royal Society of Chemistry [year]